Electronic Supplementary Material (ESI) for RSC Advances.

Supporting Information

for

A water soluble copper(II) complex as a HSO_4^- ion selective turn-on fluorescent sensor applicable in living cell imaging†

*Buddhadeb Sen, Manjira Mukherjee, Siddhartha Pal, Supriti Sen and Pabitra Chattopadhyay**

Department of Chemistry, Burdwan University, Golapbag, Burdwan, 713104, India

Corresponding author: pabitracc@yahoo.com

CONTENTS

Experimental section

Materials and physical measurements

High-purity HEPES [*4-(2-hydroxyethyl)-1-piperazine-ethane-sulfonic acid*], *2-(2-aminophenyl)benzimidazole* and *2-hydroxy-benzaldehyde* were purchased from Sigma Aldrich (India), $CuCl_2$ and *sodium hydrogen sulphate* were purchased from Merck. Other chemicals, sodium perchlorate, disodium hydrogen arsenate, tetra butyl ammonium salt of chloride, bromide, iodide, acetate, fluoride, dihydrogen phosphate and sodium hydrogen sulphate; nitrate salts of sodium, potassium, copper(II), chromium(III), silver(I), acetate salt of manganese(II), zinc(II), chloride salts of nickel(II), cobalt(II), mercury(II), calcium (II), magnesium(II), iron(III), iron(II) were of analytical reagent grade and used without further purification except when specified. Milli-Q, 18.2 MΩ cm^{-1} water was used throughout all experiments. All of the solvents were of analytical grade.

The elemental analyses (C, H and N) were performed on a Perkin Elmer 2400 elemental analyzer. Copper analysis was carried out by Varian atomic absorption spectrophotometer (AAS) model-AA55B, GTA. A Shimadzu (model UV-1800) spectrophotometer was used for recording electronic spectra. ^{1}HNMR spectrum of organic moiety was obtained on a Bruker Avance DPX 300 spectrometer using DMSO-d_6 solution. Electrospray ionization (ESI) mass spectra were recorded on a Qtof Micro YA263 mass spectrometer. A Systronics digital pH meter (model 335) was used to measure the pH of the solution and the adjustment of pH was done using either 50 mM HCl or NaOH solution. Steady-state fluorescence emission and excitation spectra were recorded with a Hitachi-4500 spectrofluorimeter. Time-resolved fluorescence lifetime measurements were performed using a HORIBA JOBIN Yvon picosecond pulsed diode laser-based time-correlated single-photon counting (TCSPC) spectrometer from IBH (UK) at λ_{ex}= 377 nm and MCP-PMT as a detector. Emission from the sample was collected at a right angle to the direction of the excitation beam maintaining magic angle polarization (54.71). The full width at half-maximum (FWHM) of the instrument response function was 250 ps, and the resolution was 28.6 ps per channel. Data were fitted to multi exponential functions after de convolution of the instrument response

function by an iterative re convolution technique using IBH DAS 6.2 data analysis software in which reduced w2 and weighted residuals serve as parameters for goodness of fit. Redox potentials were measured in CHI620D potentiometer in DMF using TBAP as supporting electrolyte at room temperature. X-band EPR spectra were taken on the Bruker EMX EPR spectrometer with a variable temperature liquid nitrogen cryostat.

The pH study was done in 1 mM HEPES buffer solution by adjusting pH with HCl or NaOH. The stock solutions (~ 10^{-2} M) for the selectivity study of the probe (**1)** towards different anions and cations were prepared taking sodium perchlorate, disodium hydrogen arsenate, tetra butyl ammonium salt of chloride, bromide, iodide, acetate, fluoride, dihydrogen phosphate and sodium hydrogen sulphate; nitrate salts of Na^+, K^+, Cu^{2+}, Cr^{3+}, Ag^+, acetate salt of Mn^{2+}, Zn^{2+}, chloride salts of Ni^{2+}, Co^{2+}, Hg^{2+}, Ca^{2+}, Mg^{2+}, Fe^{3+} ions and Fe(II)sulphate to the above solvent. In this selectivity study, the amounts of these anions were taken hundred times greater than that of the receptor. Fluorescence titration of **1** was performed with $NaHSO_4$. All the fluorescence and absorbance spectra were taken after 15 minutes of mixing of the components to acquire the optimised spectra.

Synthesis of 2-(5,6-dihydro-benzo[4,5]imidazo[1,2-c]quinazolin-6-yl)-phenol (**HL**)

A methanolic solution of *2-(2-aminophenyl)benzimidazole*, (2.09 g, 10.0 mmol) was added to the solution of *2-hydroxy-benzaldehyde* (1.22 g, 10.0 mmol) in methanol (25 mL) at room temperature with stirring. The resulting mixture was then allowed to reflux for 6.0 h. A crystalline precipitate of the compound (HL) was obtained from the yellow colored solution through slow evaporation of the solvent (Scheme S1). Pale yellow colored rectangular shaped single crystals of (HL) suitable for X-ray crystallography were obtained on slow evaporation of the DMF-methanol mixture solution.

HL. $C_{20}H_{15}N_3O$: Anal. Found: C, 76.89; H, 4.95; N, 13.17; Calc. C, 76.66; H, 4.82; N, 13.41. ESI-MS: $[M + H]^+$, m/z, 314.3490 (100 %) (Fig. S1 ESI†**)** (calcd.: m/z, 314.12; where M = molecular weight of HL]; ^{1}H NMR (δ, ppm in DMSO-d_6): 10.26 (s, 1H, O-H) 7.96 (dd, 1H); 7.65 (d, 1H); 7.31-7.23 (m, 4H); 7.20-7.11 (m, 2H); 6.87-6.73 (m, 3H); 6.60 (dd, 1H); 6.44 (dd, 1H); 4.40 (s, 1H, N-H) (Fig. S2 ESI†). Yield: 90%.

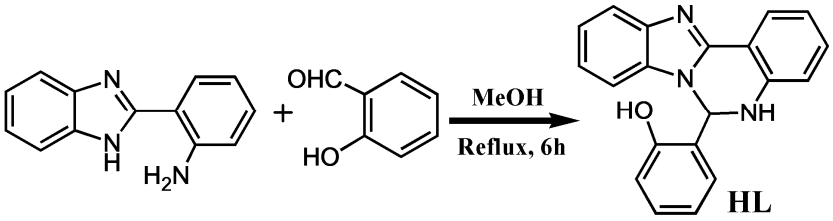

Scheme S1 Synthetic pathway of the organic moiety HL.

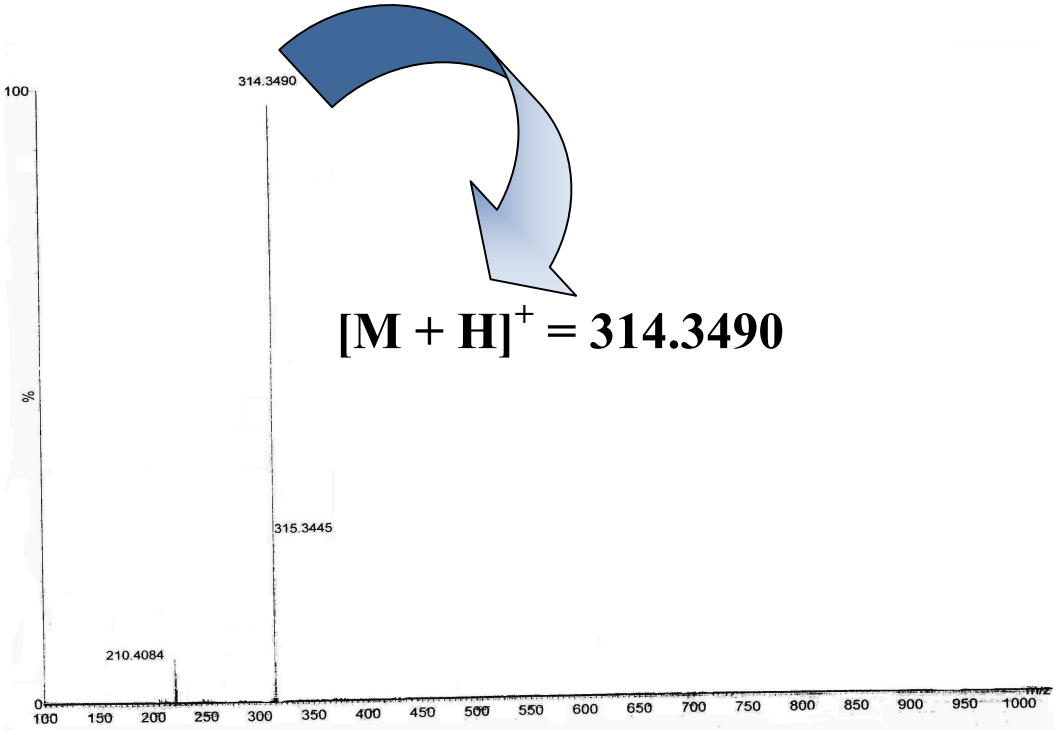

Fig. S1 ESI-MS spectrum of HL

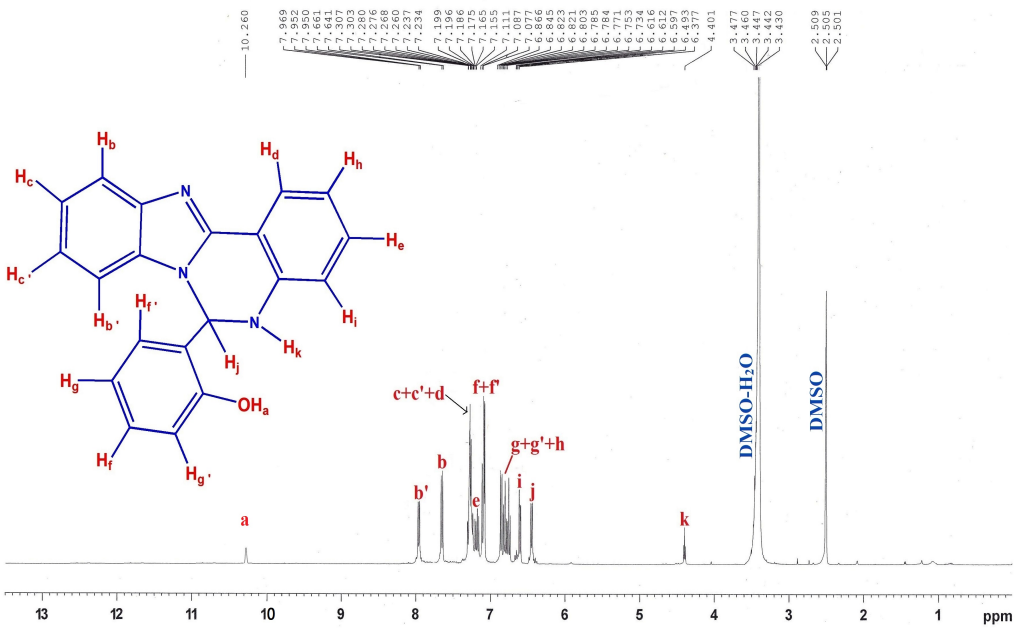

Fig. S2 ^{1}H NMR of the HL in DMSO-d_6

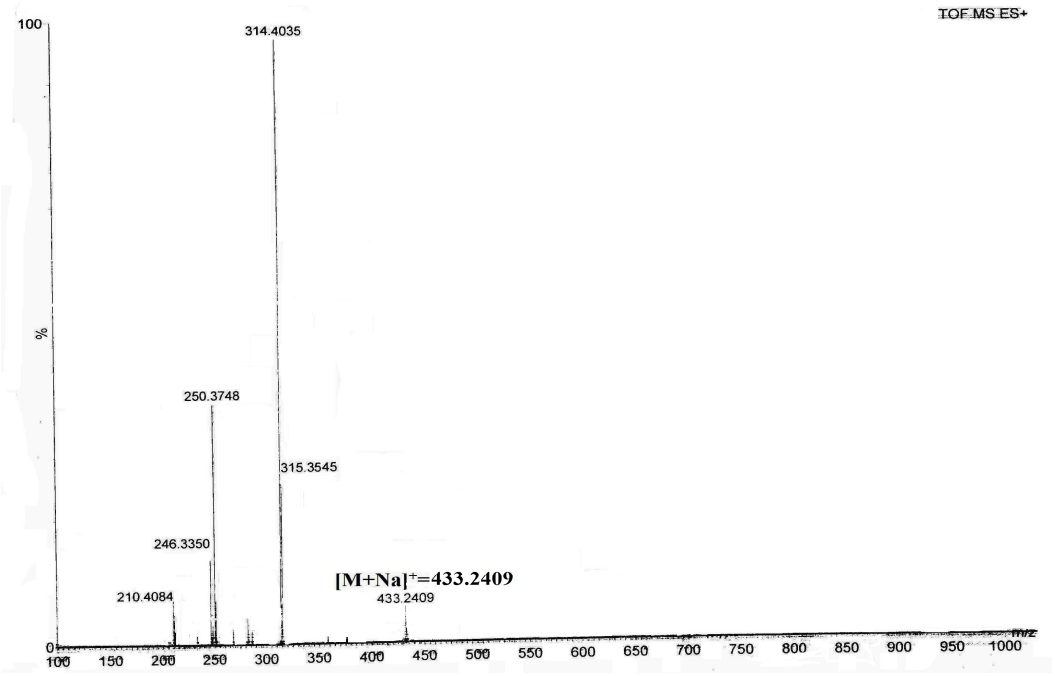

Fig. S3 ESI-MS spectrum of the probe (complex-**1)**

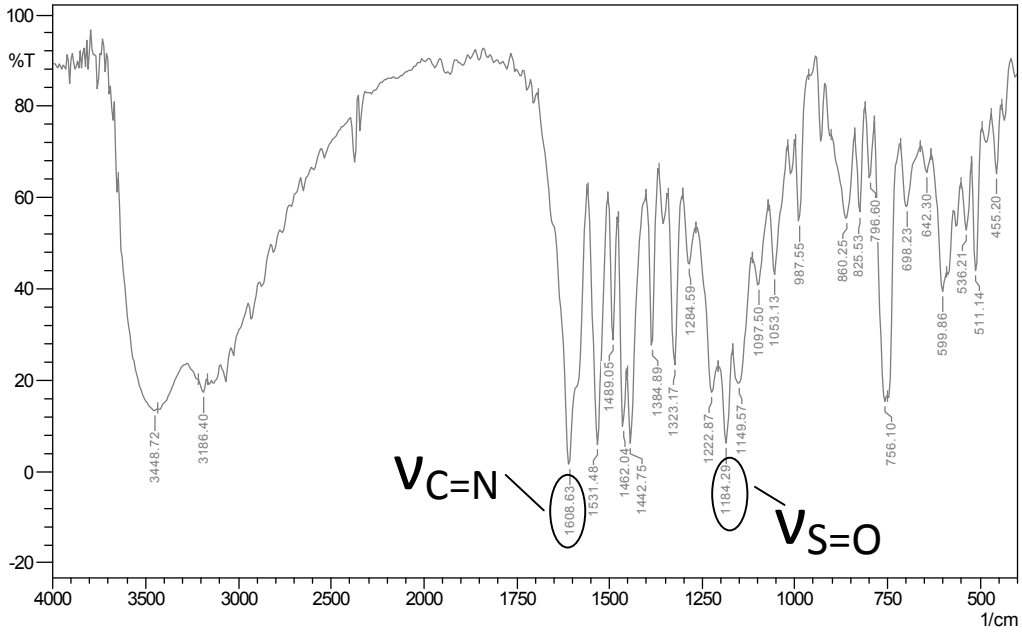

Fig. S4 IR spectrum of **1**.$NaHSO_4$ adduct

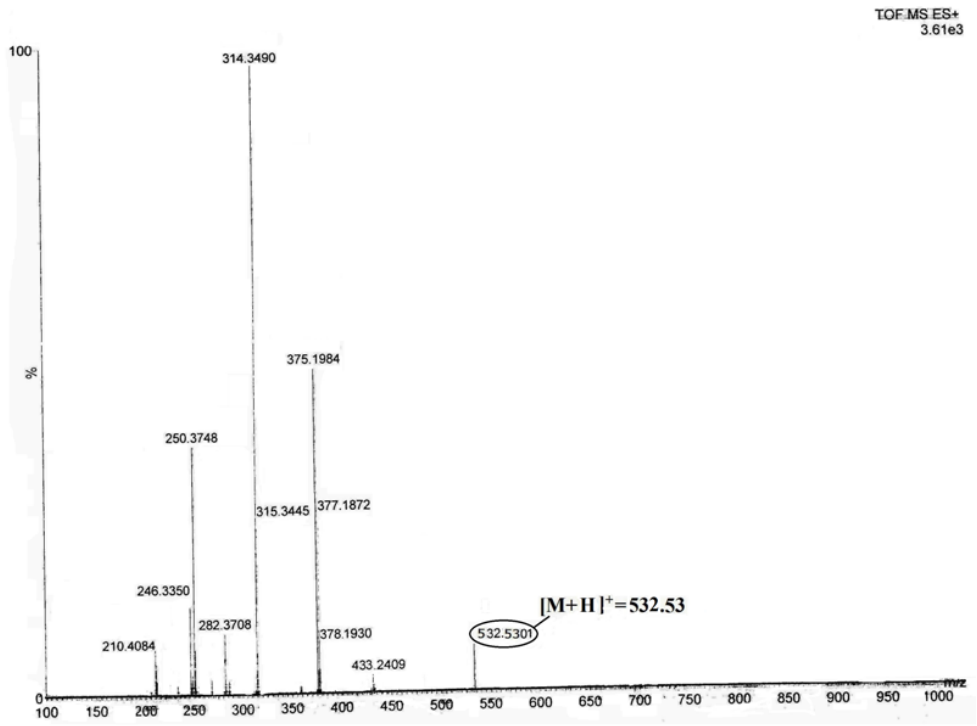

Fig. S5 ESI-MS spectrum of **1**.$NaHSO_4$ adduct

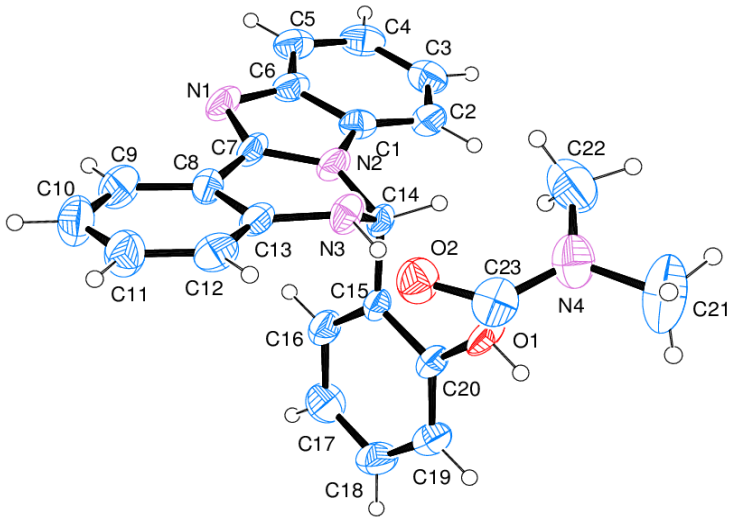

Fig. S6 An ORTEP view (30% probablity) with atom numbering scheme of HL.NMe_2CHO.

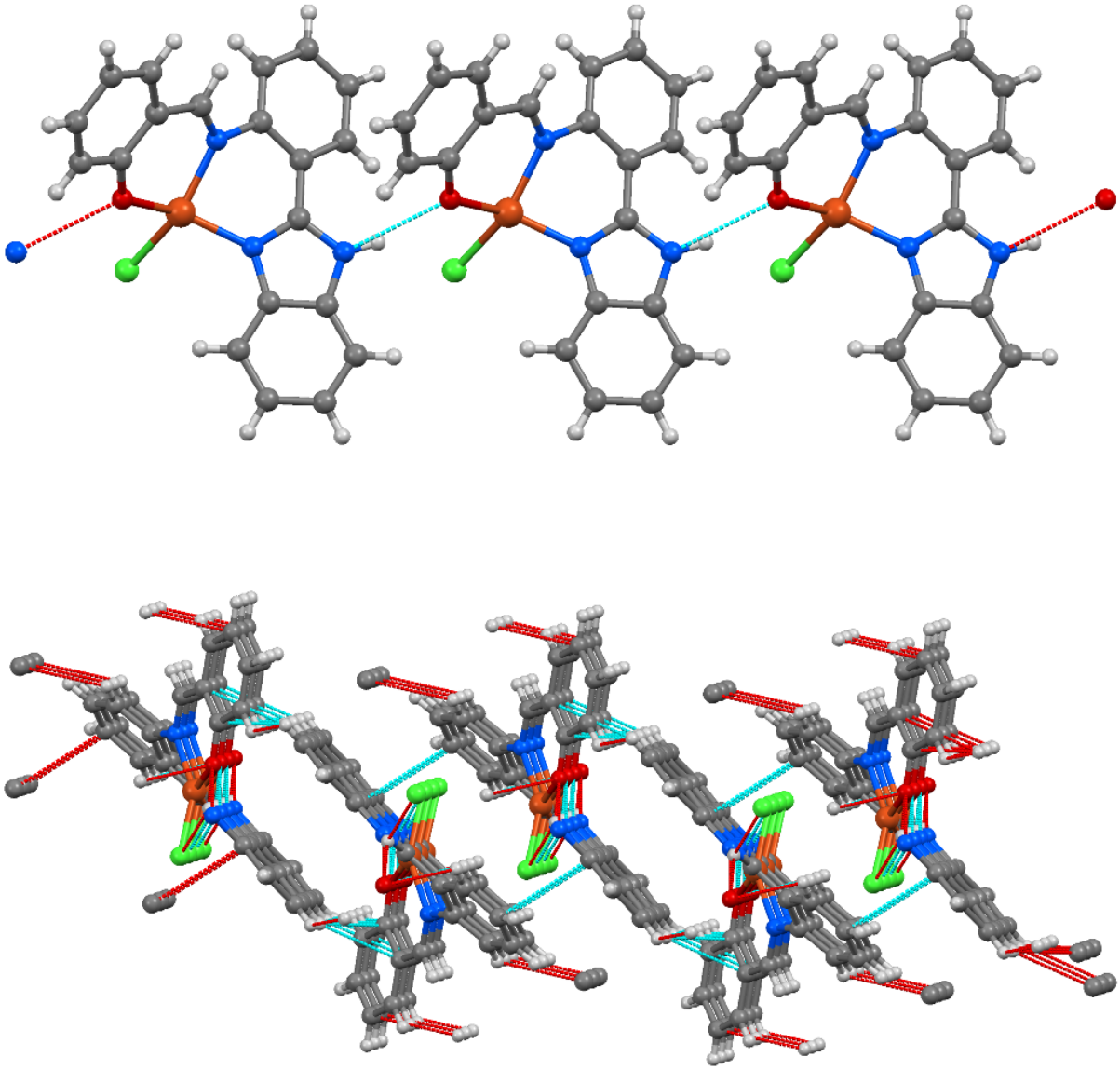

Fig. S7 Crystal packing of complex-**1** due to hydrogen bonds along with some other weaker interactions (π…π, C-H…π) are responsible for the crystal packing forming a 1D chain and 2D layered arrangement.

Scheme S2 Plausible mechanism of hydrogen sulphate sensing.

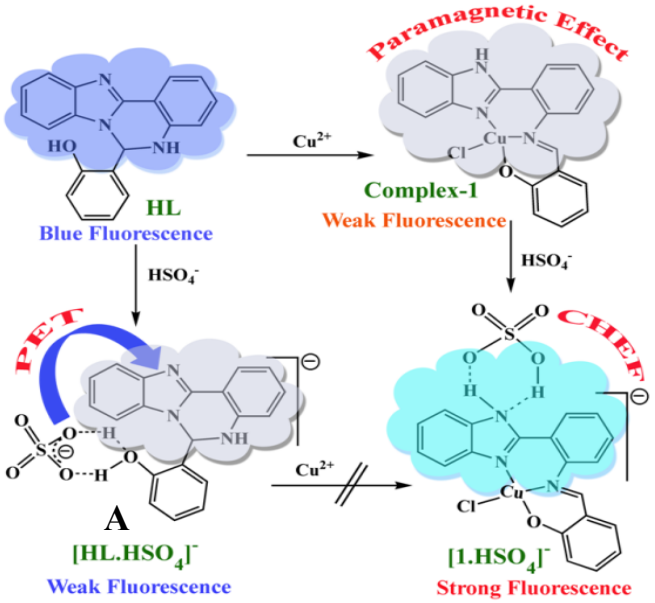

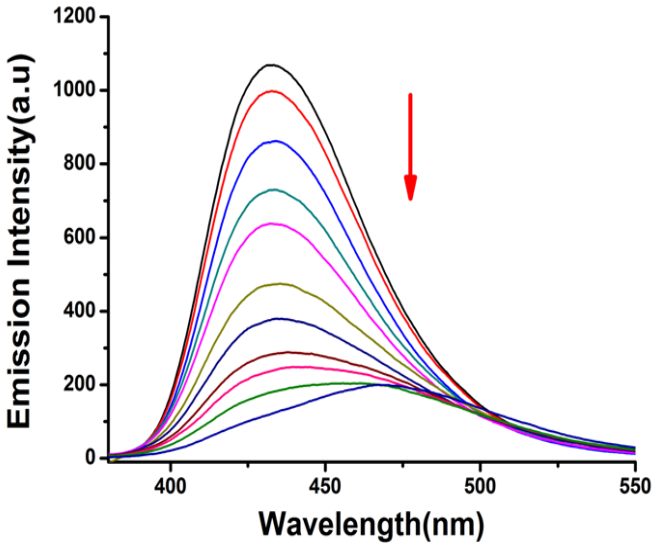

Fig. S8 Emission spectra of **HL** (10 μM) on gradual addition of HSO_4^- ions (50 μM) in DMSO: water (1:9) HEPES buffer (1 mM, pH 7.4) at 25 ^oC.

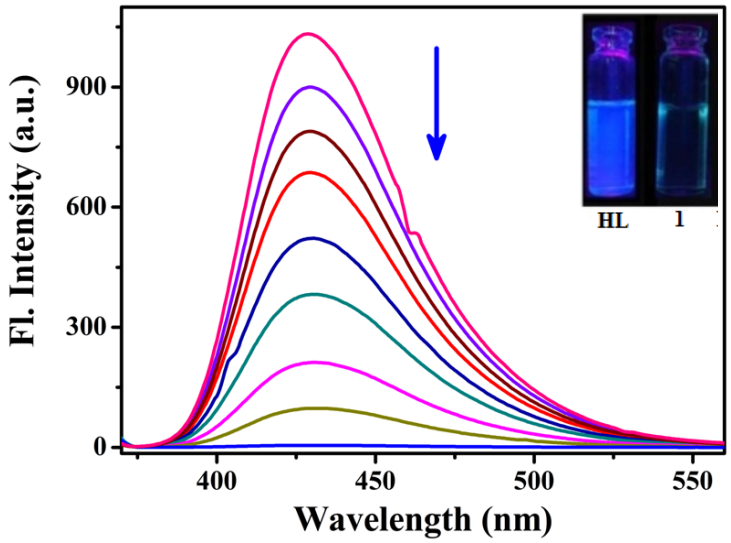

Fig. S9 Emission spectra of **HL** (10 µM) on gradual addition of Cu^{2+} ions (upto 50 µM) in DMSO: water (1:9) at 25 ^{o}C (λ_{ex}= 390 nm).

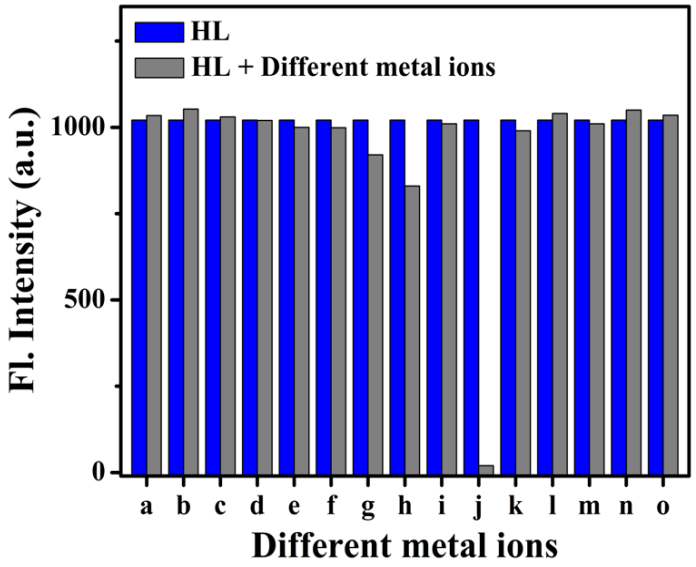

Fig. S10 Relative Fluorescence emission intensity assay of **HL** (10 µM) in presence of different metal ion salts in HEPES buffer (1 mM, pH 7.4) at 25 °C (λ_{ex} = 390 nm) where a) Na^{+}, b) K^{+}, c) Ca^{2+}, d) Mg^{2+}, e) Cr^{3+}, f) Mn^{2+}, g) Fe^{3+}, h) Co^{2+}, i) Ni^{2+}, j) Cu^{2+}, k) Zn^{2+}, l) Cd^{2+}, m) Hg^{2+}, n) Al^{3+}, and o) Pb^{2+} at λ_{em} = 430 nm.

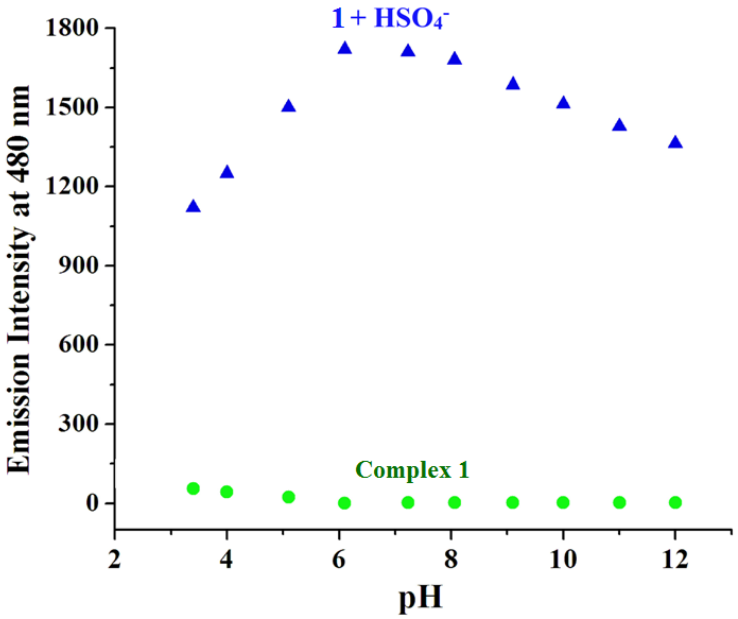

Fig. S11 Fluorescence response of complex **1** (10 μM) and **1** (10 μM) in presence of HSO_4^- ions (10 μM) in aqueous DMSO: water (1:9) media at different pH at λ_{em}= 480nm.

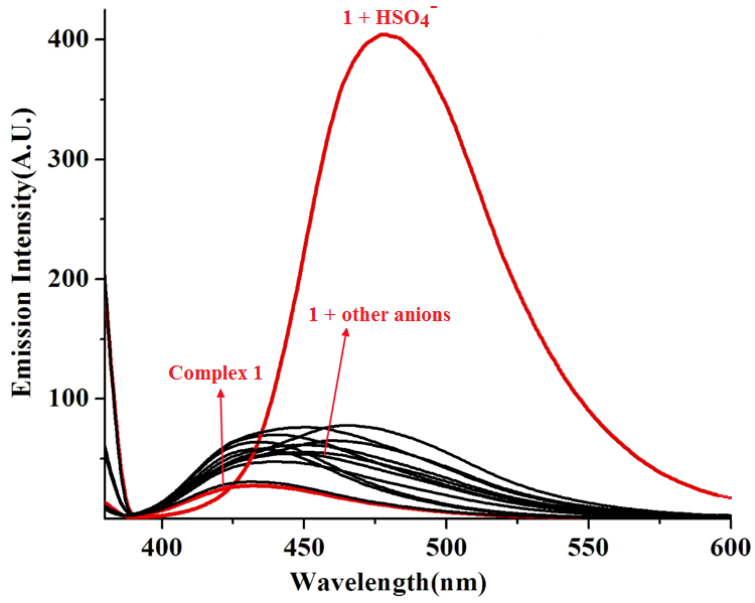

Fig. S12 Anion selectivity of complex **1** (10 μM) in presence of different anions (1000 μM) in DMSO: water (1:9).

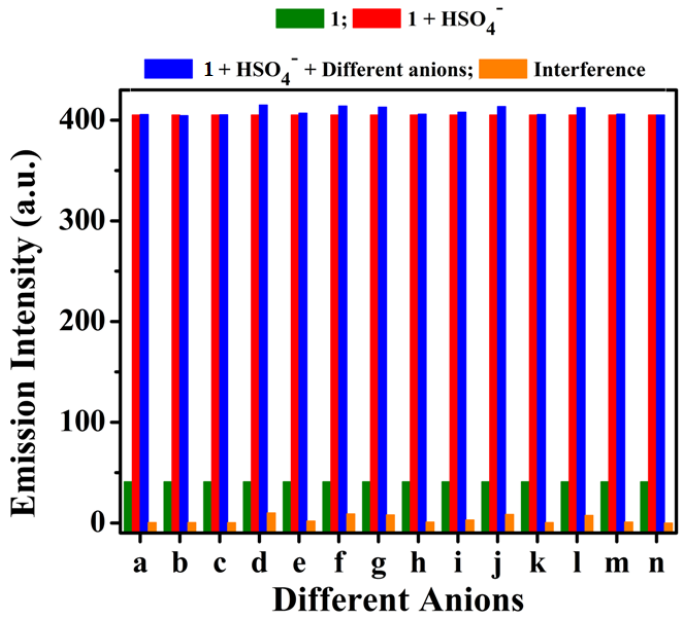

Fig. S13 Interference of different anions (50 μM) in presence of complex **1** (5.0 μM) and HSO_4^- (5.0 μM) in DMSO: water (1:9) at 25 ^oC where a) F^-, b) OAc^-, c) I^-, d) Br^-, e) N_3^-, f) CN^-, g) NO_3^-, h) ClO_4^-, i) HPO_4^{2-}, j) $H_2PO_4^-$, k) $H_2AsO_4^-$, l) Cl^-, m) HCO_3^-, n) SO_4^{2-} at λ_{em}= 480nm.

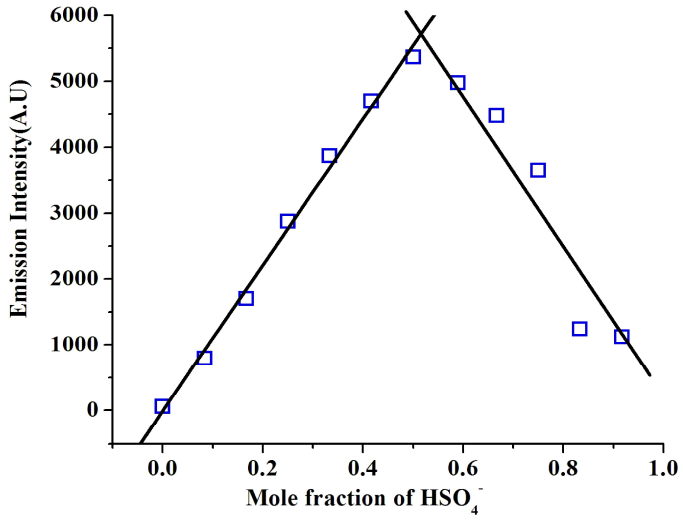

Fig. S14 Job's plot for stoichiometry determination between complex **1** (10 μM) and HSO_4^- ions in DMSO: water (1:9) at 25 ^oC from the emission data at λ_{em}= 480nm.

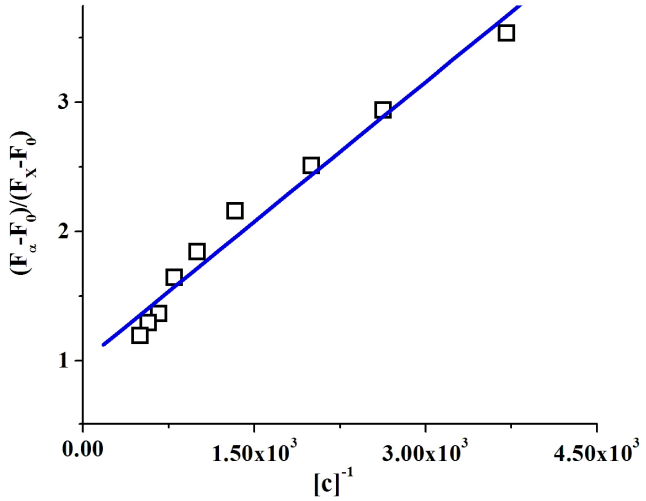

Fig. S15 Binding constant (K_a) value 1.4×10^5 M^{-1} determined from the interaction of complex **1** with HSO_4^- ions considering the emission data.

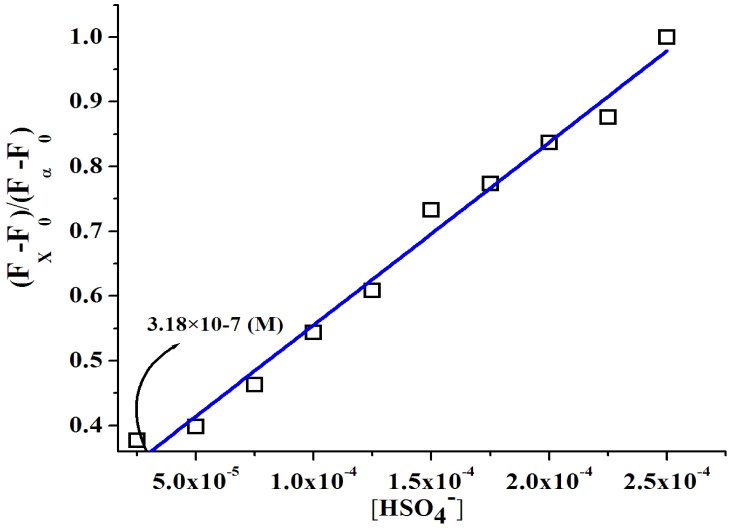

Fig. S16 Detection limit of HSO_4^- ions (3.18×10^{-7} M) in DMSO: water (1:9) at 25 ^oC at λ_{em}= 480nm.

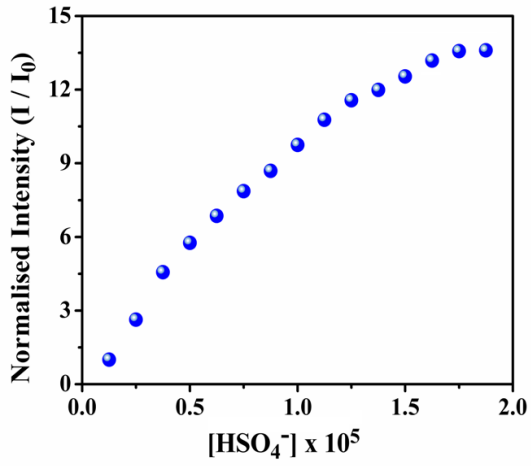

Fig. S17 Calibration graph of linearity range ($3.18x10^{-7}$ to $1.25x10^{-5}$) for the detection of HSO_4^- ions in DMSO: water (1:9) at 25 ^oC.

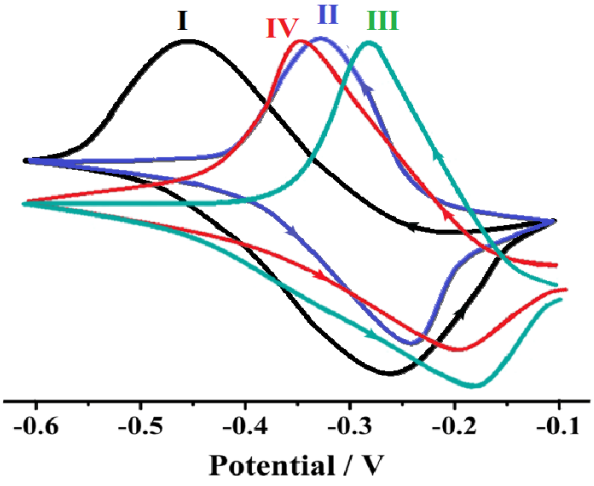

Fig. S18 Cyclic voltammogram (scan rate 100 mV/s) of complex **1** (I) and **1**.HSO_4^- adduct (II) **1** in presence of HCl (III) and **1** + HCl + SO_4^{2-} (IV) in DMF solution containing 0.1 M TBAP, using platinum working electrode.

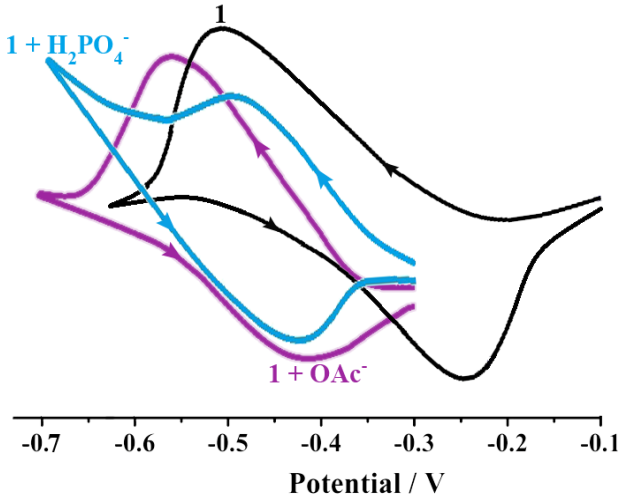

Fig. S19 Cyclic voltammogram (scan rate 100 mV/s) of complex **1**, **1** in presence of $H_2PO_4^-$ ions and **1** in presence of OAc^- ions in DMF solution containing 0.1 M TBAP, using platinum working electrode.

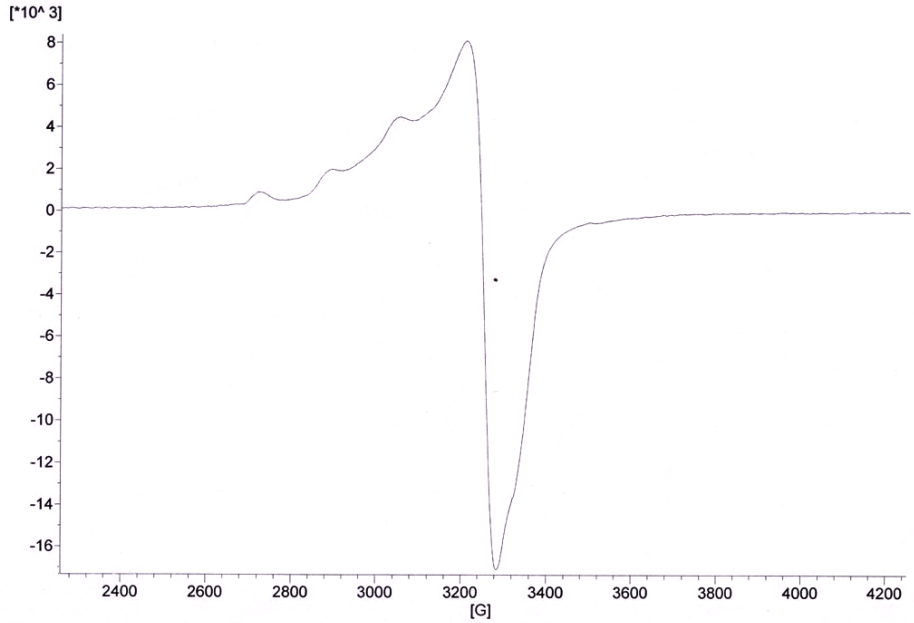

Fig. S20 EPR spectrum of the complex-**1** in methanol at 120 K.

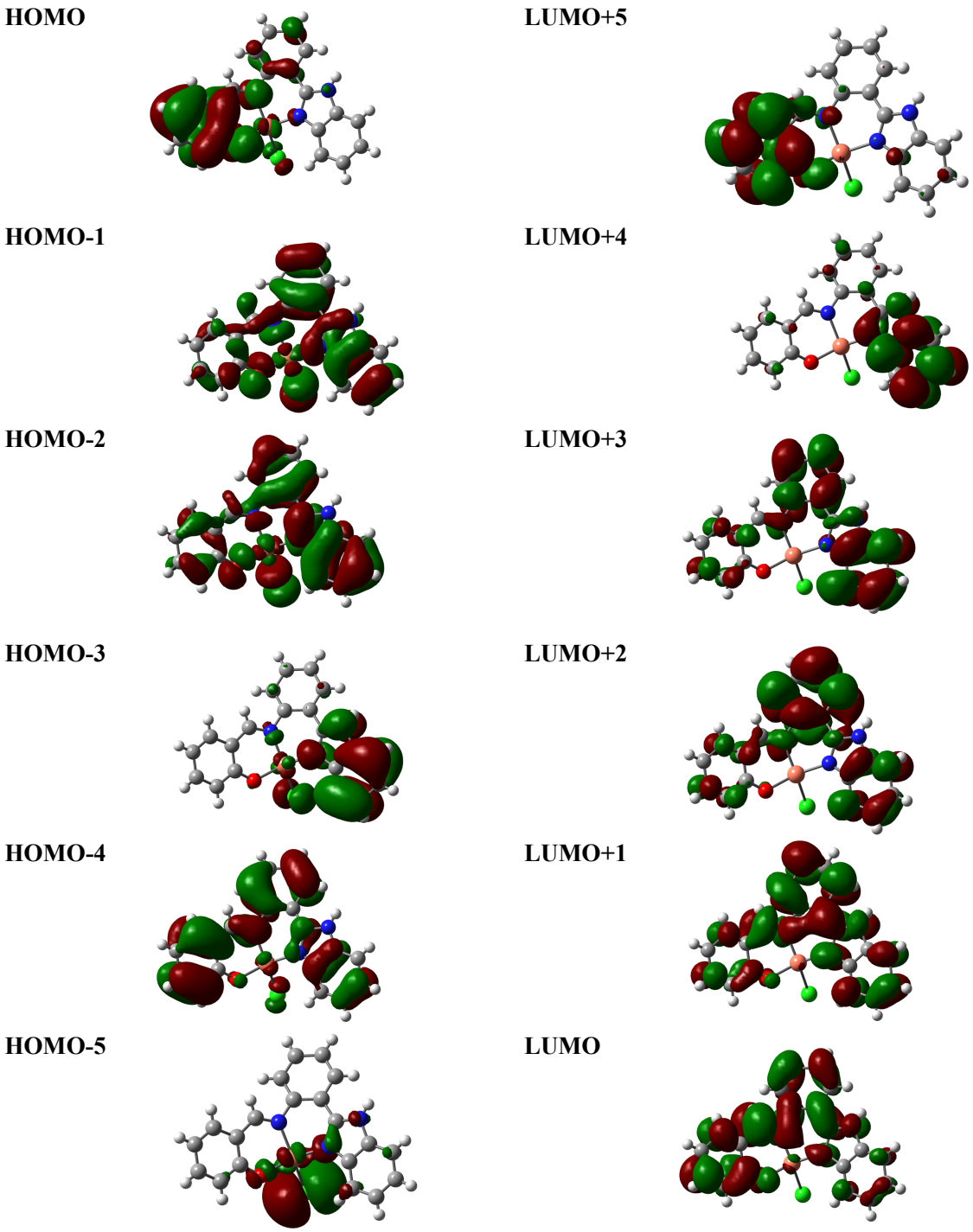

Fig. S21 Some HOMO and LUMO's of complex **1**

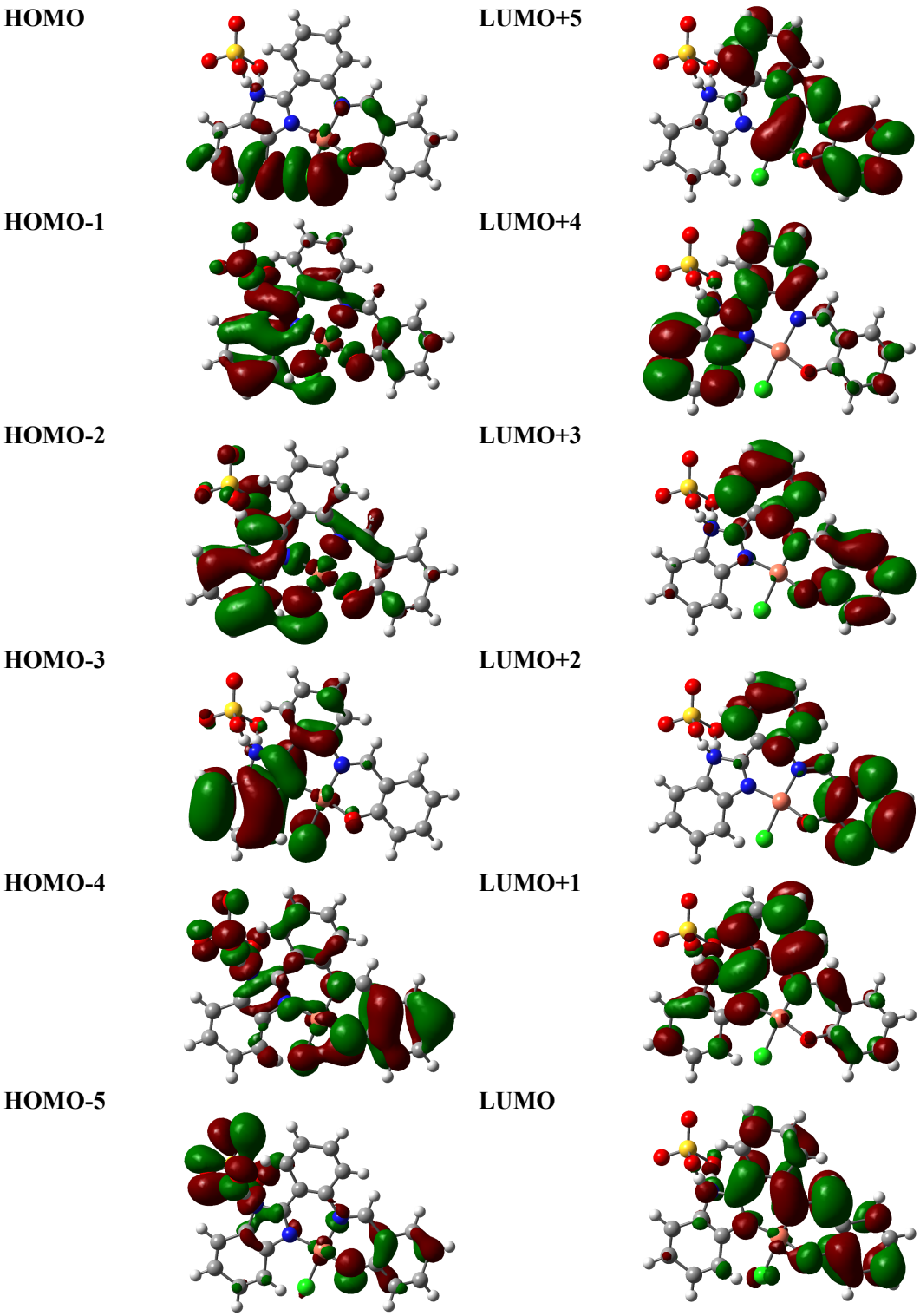

Fig. S22 Some HOMO and LUMO's of **1.**HSO_4^- adduct

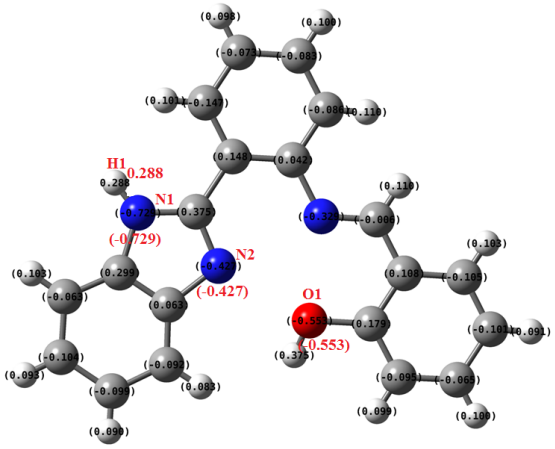

HL′

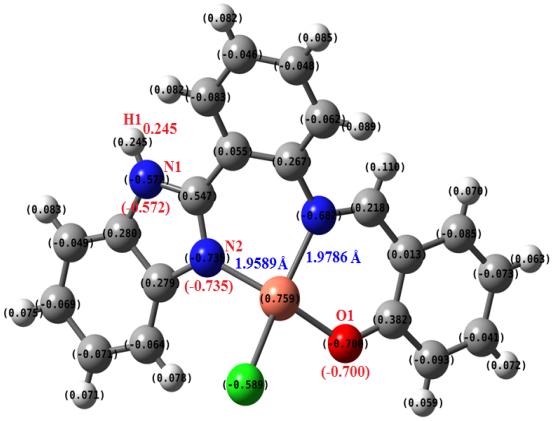

Complex 1

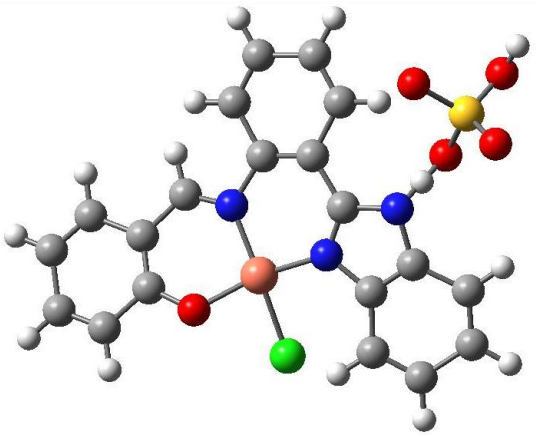

1.HSO_4^- (Linear)

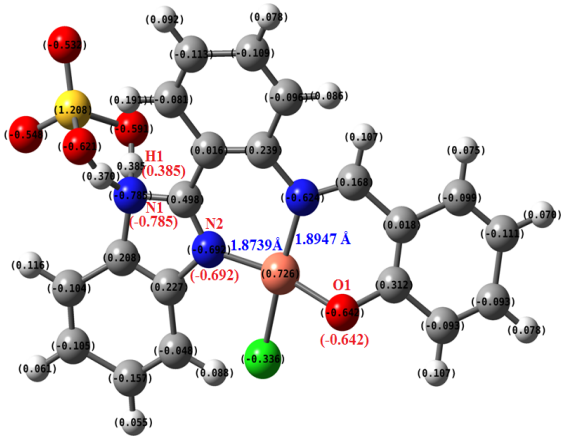

1.HSO_4^- (Ring)

Fig. S23 Optimized structures of HL′, Complex **1**, **1**.HSO_4^- (Linear) and **1**.HSO_4^- (Ring) along with the NPA charge distribution.

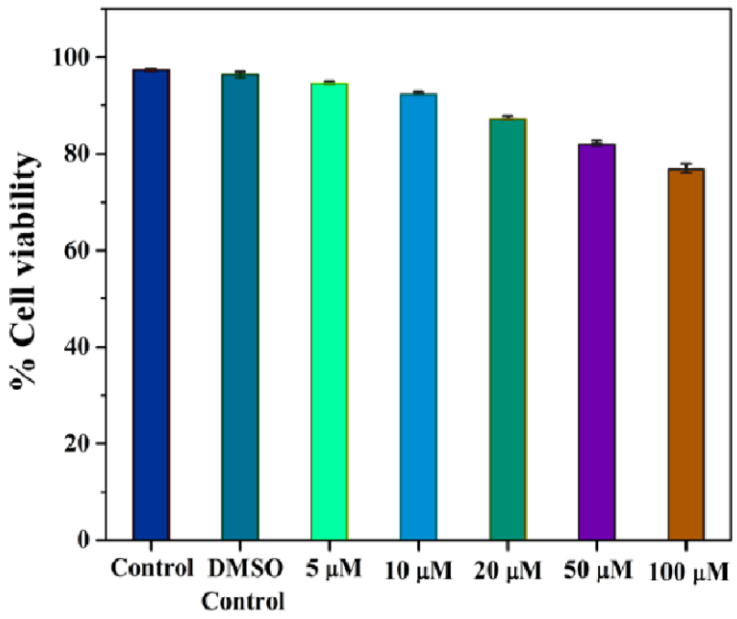

Fig. S24 Cytotoxic effect of complex **1** (5, 10, 20, and 50 μM) in HeLa cells incubated for 12 h by MTT assay. Results are expressed as mean of three independent experiments.

Table S1 Crystal data and details of refinements for HL.NMe_2CHO and [Cu(L′)(Cl)] (**1**)

	HL.NMe_2CHO	Complex **1**
Empirical Formula	C_{23} $H_{22}N_4O_2$	$C_{20}H_{14}ClCuN_3O$
Formula Weight	386.45	411.33
Crystal System	Monoclinic	Triclinic
Space group	Cc	P-1
a (Å)	14.7508(11)	8.06690(10)
b (Å)	9.8446(8)	10.2015(2)
c (Å)	13.9881(8)	10.8792(2)
α (^{o})	90	90.4250(10)
β (^{o})	91.028(3)	104.9720(10)
γ (^{o})	90	94.3570(10)
Density (calculated)	1.264	1.585
Volume (Å^3)	2031.0(3)	862.07(3)
Temperature, K	293(2) K	296(2)
Z	4	2
F (000)	816	418
θ range(deg)	2.49 to 22.92	2.75 to 28°
Collected reflections	5292	15679
Independent reflections	2413 [R(int) = 0.0249]	4147
Goodness-of-fit	0.942	1.028
R1 [I > 2.0 σ(I)]	0.0402	0.0364
wR1 [I > 2.0 σ(I)]	0.1057	0.0892

Table S2 Selected bond distances (Å) and bond angles (°) for HL.NMe_2CHO

Bond distances (Å)			
C13-N3	1.395(5)	C20-O1	1.356(5)
C14-N3	1.463(5)	C1-C6	1.381(5)
C14-N2	1.461(4)	C7-C8	1.473(5)
C7-N1	1.302(5)	C14-C15	1.515(5)
C7-N2	1.354(4)	C8-C13	1.398(5)
C23-N4	1.318(6)	C23-O2	1.220(5)
Bond angles (°)			
N1-C7-N2	114.1(4)	N3-C14-C15	112.8(3)
N2-C7-C8	117.6(3)	N2-C1-C6	104.5(3)
C8-C13-N3	117.9(3)	C16-C15-C20	118.4(3)
C13-N3-C14	118.8(3)	C6-C1-C2	122.7(4)
N3-C14-N2	105.5(3)	C12-C13-C8	119.5(3)
O1-C20-C15	115.8(3)	O2-C23-N4	127.0(4)
C1 N2 C14	128.9(3)	C22-N4-C23	120.7(4)

Table S3 Selected bond distances (Å) and bond angles (°) for complex-**1**

Bond distances (Å)			
C7-N3	1.336(3)	C16-O1	1.311(3)
C8-N2	1.374(3)	C1-C2	1.413(3)
C7-N2	1.354(3)	C15-C16	1.418(3)
C1-N1	1.430(3)	Cu1-N1	1.9786(19)
C14-N1	1.296(3)	Cu1-N3	1.9591(18)
C14-C15	1.426(3)	Cu1-O1	1.9093(16)
C8-C9	1.405(3)	Cu1-Cl1	2.2425(7)
Bond angles (°)			
N3-C7-N2	111.2(2)	N1-C14-C15	127.5(2)
N2-C8-C9	106.0(2)	N1-Cu1-O1	94.03(7)
C2-C7-N3	125.8(2)	C15-C16-O1	123.5(2)
C7-N3-Cu1	123.86(16)	C14-C15-C16	123.6(2)
N1-C1-C2	119.9(2)	C2-C1-C6	119.4(2)
C7-N3-C9	106.31(18)	C8-C9-C10	120.6(2)
C1-N1-Cu1	120.17(15)	C15-C16-C17	117.3(2)

Table S4 $E_{1/2}$ values of complex-**1** in presence of different ions

Composition	*ca.* $E_{1/2}$ (*vs*. Ag/AgCl)
Complex-**1**	-0.38 V
1 + HSO_4^-	-0.29 V
1 + HCl	-0.23 V
1 + HCl + SO_4^{2-}	-0.28 V
1 + $H_2PO_4^-$	-0.46 V
1 + OAc^-	-0.49 V
1 + F^- / CN^-	-0.39 V

Table S5 HOMO-LUMO energy of Complex-**1**, **1.**HSO_4^- (path-A) and **1.**HSO_4^- (path-B)

Component	HOMO (eV)	LUMO (eV)	Difference (eV)
Complex-**1**	-5.7606	-2.0881	3.6725
1-HSO_4^- (Linear) (path-A)	- 4.6327	-1.7404	2.8923
1-HSO_4^- (Ring) (path-B)	-4.7465	-2.3082	2.4383

Table S6 HOMO-LUMO energy of Complex-**1**, **1**-HSO_4^- adduct (Ring)

Complex-**1**		1.HSO_4^- ensemble (Ring)	
MO's	Energy (eV)	MO's	Energy (eV)
LUMO+5	0.9213	LUMO+5	0.2569
LUMO+4	0.3643	LUMO+4	0.0416
LUMO+3	0.3140	LUMO+3	-0.1513
LUMO+2	-0.2628	LUMO+2	-0.3815
LUMO+1	-1.5349	LUMO+1	-1.4062
LUMO	-2.0881	LUMO	-2.3082
HOMO	-5.7606	HOMO	-4.7465
HOMO-1	-6.3046	HOMO-1	-5.6594
HOMO-2	-6.4743	HOMO-2	-5.9321
HOMO-3	-6.6969	HOMO-3	-6.1767
HOMO-4	-6.8354	HOMO-4	-6.3081
HOMO-5	-7.1409	HOMO-5	-6.7601

Table S7 Vertical excitation energies (E_{ex}), oscillator strengths (f), and Key transitions of the lowest few excited singlets obtained from TDDFT calculations of complex-**1** in H_2O

$E_{excitation}$ (eV)	$\lambda_{excitation}$ (nm)	Osc. strength (f)	Key transitions	CI	$\lambda_{expt.}$ (nm)
2.7879	444.72	0.0154	HOMO→ LUMO HOMO→ LUMO+1	0.62613 0.35022	
2.9516	420.05	0.0014	HOMO-1 → LUMO+1 HOMO-1 → LUMO	0.39953 0.48273	
3.1196	397.43	0.1464	HOMO → LUMO HOMO → LUMO+1	0.66109 0.66289	403
3.2510	381.37	0.0011	HOMO-2 → LUMO+1 HOMO-1 → LUMO+1 HOMO-3 → LUMO HOMO-1 → LUMO+2	0.25411 0.26693 0.28672 0.37261	
3.2742	378.67	0.0148	HOMO-1 → LUMO HOMO-3 → LUMO+1	0.72998 0.14366	
3.3773	367.11	0.0058	HOMO-2 → LUMO HOMO-1 → LUMO HOMO-1 → LUMO+1	0.27510 0.68172 0.31193	
3.8217	346.42	0.2276	HOMO-1 → LUMO+2 HOMO-1 → LUMO+1	0.36965 0.63372	
3.6589	338.86	0.0121	HOMO → LUMO+1 HOMO → LUMO+2	0.70978 0.54503	
3.7466	330.92	0.0237	HOMO-4 → LUMO HOMO-1 → LUMO+1	0.34543 0.21471	
3.9610	313.01	0.0235	HOMO-1 → LUMO+1 HOMO-4 → LUMO+1	0.58576 0.16163	315

Table S8 Vertical excitation energies (E_{ex}), oscillator strengths (f), and Key transitions of the lowest few excited singlets obtained from TDDFT calculations of **1.HSO_4^-** adduct in H_2O

$E_{excitation}$ (eV)	$\lambda_{excitation}$ (nm)	Osc. strength (f)	Key transitions	CI	$\lambda_{expt.}$ (nm)
1.9368	640.14	0.0150	HOMO → LUMO+1	0.75351	
2.5463	486.92	0.0060	HOMO- 1 → LUMO HOMO- 2 → LUMO HOMO- 3 → LUMO	0.42705 0.28939 0.19760	
3.0222	410.25	0.2178	HOMO- 1 → LUMO HOMO- 2 → LUMO HOMO- 3 → LUMO	0.63511 0.59143 0.32879	403
3.1593	392.44	0.0026	HOMO-4 → LUMO HOMO- 1 → LUMO+1	0.43603 0.15788	
3.2196	385.09	0.0409	HOMO- 2 → LUMO HOMO- 3 → LUMO	0.63979 0.63751	
3.3724	367.65	0.0059	HOMO- 1 → LUMO+1 HOMO- 3 → LUMO HOMO- 4 → LUMO	0.46003 0.55291 0.26595	
3.4275	361.74	0.0156	HOMO- 1 → LUMO+1 HOMO- 3 → LUMO HOMO- 4 → LUMO HOMO- 2 → LUMO+1	0.15746 0.15247 0.39940 0.12779	
3.4676	357.55	0.0626	HOMO- 1 → LUMO+1 HOMO- 2 → LUMO+1	0.45191 0.20431	
3.8121	325.24	0.0655	HOMO → LUMO+2 HOMO- 2 → LUMO+1 HOMO- 5 → LUMO	0.51451 0.29795 0.51463	
3.8235	324.27	0.0713	HOMO- 3 → LUMO+1 HOMO- 4 → LUMO HOMO- 5→ LUMO	0.24523 0.27331 0.33968	
3.8555	321.58	0.0122	HOMO → LUMO+2 HOMO → LUMO+3 HOMO → LUMO+4	0.30880 0.69542 0.31867	305